

Optical properties of pulse electrodeposited ZnS films

K. R. Murali¹

¹ ECMS Division, CSIR-CECRI, Karaikudi, India

Abstract : ZnS films were deposited by the pulse plating technique at different duty cycles in the range of 6 – 50 % and at a constant current density of 10 mA cm⁻². The films exhibited single phase hexagonal ZnS. The grain size increased with decrease of duty cycle. Optical band gap of the films increased from 3.83 – 4.01 eV with increase of duty cycle. Optical constants (refractive index, n, extinction co-efficient, k, dielectric constant) of the films were obtained in the wavelength range 300-1850 nm by using spectrophotometric measurement. The obtained results concerning the absorption index yield the energy gap in addition to the type of the allowed optical transitions. N/m* ratio has been obtained from refractive index data. The dispersion of refractive index is analyzed by using a single oscillator model.

Keywords: electrodeposition, electronic materials, optical properties, semiconductors, thin films

I. Introduction

Zinc sulfide (ZnS) is found in nature as zinc-blende (also called sphalerite or β -ZnS and with a cubic structure) and wurtzite (α -ZnS, which is a hexagonal structure). The names of these minerals are used to designate the corresponding crystalstructures. It is a II–VI compound semiconductor material and is commercially used in solar cells [3], infrared windows [4], and phosphor materials by doping with transition or rare-earth metals [5,6]. There has been growing interest in developing techniques to prepare semiconductor ZnS thin films. ZnS thin films are produced using various techniques, including radio frequency (RF) magnetron sputtering [7], chemical vapor deposition (CVD) [8], solvothermal [9] and chemical bath deposition [10]. In an earlier paper, details of pulse plating technique at different duty cycles in the range of 20 – 60 % and the structural, morphological and band gap of the films were reported [11]. In this work, we report on the deposition of ZnS thin films at different duty cycles in the range of 6 – 50 %, using pulse electrodeposition technique. Optical properties of the films are analyzed and the optical constants were evaluated and discussed.

In pulse electrodeposition [12,13] the potential or current is alternated swiftly between two different values. This results in a series of pulses of equal amplitude, duration and polarity, separated by zero current. Each pulse consists of an ON-time (T_{ON}) during which potential and/current is applied, and an OFF-time (T_{OFF}) during which zero current is applied. It is possible to control the deposited film composition and thickness in an atomic order by regulating the pulse amplitude and width. They favor the initiation of grain nuclei and greatly increase the number of grains per unit area resulting in finer grained deposit with better properties than conventionally plated coatings. The sum of the ON and OFF times constitute one pulse cycle. The duty cycle is defined as follows:

$$\text{Duty Cycle (\%)} = (\text{ON time}) / (\text{ON time} + \text{OFF time}) \times 100 \text{ ----- (1)}$$

A duty cycle of 100% corresponds to conventional plating because OFF time is zero. In practice, pulse plating usually involves a duty cycle of 5% or greater. During the ON time, the concentration of the metal ions to be deposited is reduced within a certain distance from the cathode surface. This so-called diffusion layer pulsates with the same frequency as the applied pulse current. Its thickness is also related to i_p , but reaches a limiting value governed primarily by the diffusion coefficient of the metal ions. During the OFF time the concentration of the metal ions build up again by diffusion from the bulk electrolyte and will reach the equilibrium concentration of the bulk electrolyte if enough time is allowed. These variables result in two important characteristic features of pulse plating which make it useful for alloy plating as well as property changes as mentioned earlier.

Pulse plating technique has distinct advantages compared to conventional electrodeposition namely, crack free, hard deposits and fine grained films with more uniformity, lower porosity and better adhesion. It is well known that by using pulse current for electrodeposition of metals and alloys it is possible to exercise greater control over the properties of electrodeposits and to improve them by modifying their microstructures [14]. It has been reported that a significant reduction in internal stress could be obtained when pulse current was used, compared to the use of conventional direct current [15].

II. Materials And Methods

ZnS films were pulse electrodeposited at 10 mA cm⁻² at room temperature and at different duty cycles in the range of 6 – 50 %. Tin oxide coated glass substrates were used. The total deposition time was kept

constant at 30 min. Thickness of the films measured by Mitutoyo surface profilometer was in the range of 525 nm – 1450 nm with decrease of duty cycle. The films were characterized by Xpertanalytical x-ray diffraction unit with $\text{CuK}\alpha$ radiation. Optical measurements were recorded using an Hitachi UV–Vis-IR spectrophotometer. Composition of the films was estimated by EDS attachment to JOEL SEM.

III. Results And Discussion

Fig. 1 shows a typical XRD pattern of the ZnS film grown by pulse electrodeposition at different duty cycles. The diffraction pattern of the films revealed a polycrystalline wurtzite crystal structure and the presence of two phases corresponding to ZnS (JCPDS no. 36-1450) [16] with a strong preferred orientation along the hexagonal (110) ZnS plane direction. Other characteristic planes for hexagonal ZnS were observed as weak peaks at (100), (002), (101), (110), (103), (112) and (203). The evaluated lattice parameters were $a = 3.76 \text{ \AA}$ and $c = 24.92 \text{ \AA}$. The crystallite size was calculated from the Full width half maximum of the diffraction profiles using Scherrer's equation

$$D = 0.95 \lambda / (\beta \cos\theta) \dots\dots\dots(2)$$

where, D is the crystallite size, λ is the wavelength of $\text{CuK}\alpha$ radiation, β is the full width at half maximum, θ is the Bragg angle. The crystallite size decreased from 80 nm – 40 nm with increase of duty cycle. The crystallite size and thickness of the films are shown in Table.1. The trend of decreasing grain size with increasing current on-time can best be explained by an increased number of nucleation sites caused by the higher overpotential at longer current on-times. The same behavior of increasing overpotential with current on-time was also found during zinc deposition from a chloride-based electrolyte [17]. Moreover, at low duty cycles, the OFF time is more compared to ON time, hence, the deposited species have sufficient time to nucleate and grow thus increasing the thickness. As the duty cycle increases, the ON time increases and OFF time decreases, which was found to yield grain growth, which can be explained by both the decrease of overpotential and longer time for the adatoms to surface migrate and enhance the crystal grain-growth process, resulting in a decreased rate of nucleation and growth rate, hence, the thickness of the films decreases.

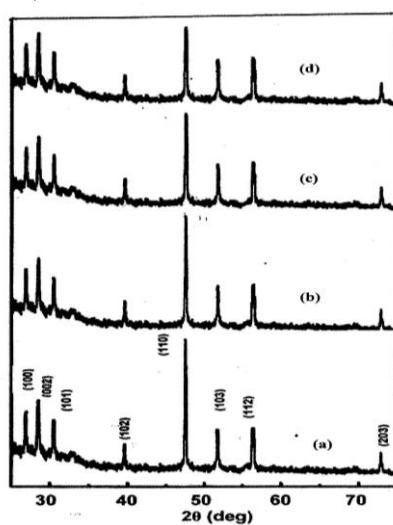


Figure.1 - XRD pattern of ZnS films deposited at different duty cycles (a) 6 % (b) 15 % (c) 33 % (d) 50 %

Table-1 Variation of crystallite size and thickness with duty cycle for ZnS films deposited at different duty cycles		
Duty cycle (%)	Cryst allite size (nm)	Thickness (nm)
6	80	1450
15	65	850
33	52	675
50	40	525

Composition of the films was determined by the Energy dispersive x-ray analysis (EDAX) attachment of the Scanning Electron Microscope (SEM). At low duty cycles, more concentration of S is deposited due to the fact that S is more noble compared to Zn. As the duty cycle is increased, due to increase of ON time, more Zn is deposited along with S, hence the percentage of Zn increases. Fig.2 shows the Energy dispersive spectrum (EDS) spectrum of ZnS films deposited at 50 % duty cycle. Table-2 shows the composition of the films deposited at different duty cycles.

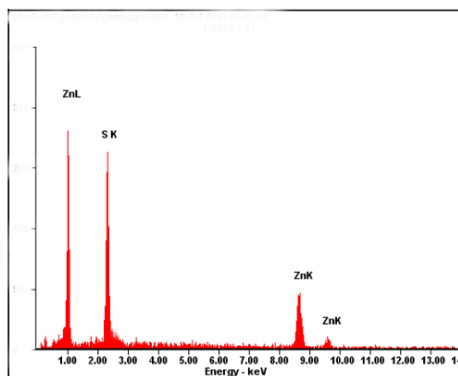


Figure.2 – EDS spectrum of ZnS films deposited at 50 % duty cycle

Table-2

Composition of ZnS films deposited at different duty cycles			
Duty cycle (%)	Zn (%)	S (%)	Zn/S
6	45.24	54.76	0.83
15	46.38	53.62	0.86
33	47.95	52.05	0.92
50	49.84	50.16	0.99

Fig.3 shows the transmission spectra of the ZnS films deposited at different duty cycles. The spectra exhibit interference fringes and the value of the refractive index was estimated by the envelope method [18] as follows:

$$n = [N + (N^2 - n_s^2)]^2 \dots\dots\dots(3)$$

$$N = (n_s^2 + 1)/2 + 2 n_s (T_{max} - T_{min}) / T_{max} T_{min} \dots\dots\dots(4)$$

where n_s is the refractive index of the substrate, T_{max} and T_{min} are the maximum and minimum transmittances at the same wavelength in the fitted envelope curve on a transmittance spectrum. The value of the refractive index at 450 nm, calculated from the above equations was in the range of 4.30 - 3.00 for the samples deposited at different duty cycle. This value is comparable to the values obtained on chemical bath deposited ZnS films [19]. Variation of refractive index with wavelength is shown in Fig.4.

The value of the absorption co-efficient (α) was calculated using the relation $\alpha = 1/d \ln \{ (n-1)(n-n_s)/(n+1)(n-n_s) \} [(T_{max}/T_{min})^2 + 1] / [(T_{max}/T_{min})^2 - 1] \dots\dots\dots(5)$

where 'd' is the thickness of the film and the other parameters have the usual meaning as given for equation (4). The films exhibited a high absorption co-efficient of the order of 10^4 cm^{-1} . A plot of $(\alpha h\nu)^2$ against $h\nu$, as indicated in Fig. 5, exhibits linear behavior near the band edge, the band gap of the deposited films was determined to be in the range of 3.83 – 4.01 eV. The band gap slightly increased with increase of duty cycle, due to the decrease of grain size. The band gap of ZnS thin film prepared by chemical bath deposition technique was in the range of 3.70 eV -4.01 eV [19]. Extinction coefficient was determined from the absorption coefficient using the following relation. Fig.6 shows the variation of extinction coefficient with wavelength.

$$k = \alpha\lambda/4\pi \dots\dots\dots(6)$$

where α is the absorption coefficient and λ is the wavelength. As seen from the figure, the extinction coefficient decreases with the increase in the wavelength. The decrease in extinction coefficient with increase in wavelength shows that the fraction of light lost due to absorbance decreases

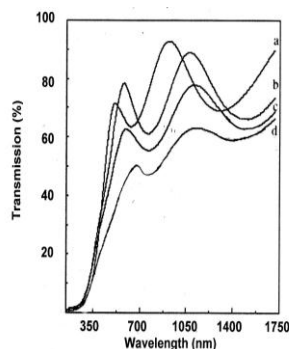


Figure.3 – Transmission spectra of ZnS films deposited at different duty cycles (a)50% (b) 33% (c) 15% (d) 6 %

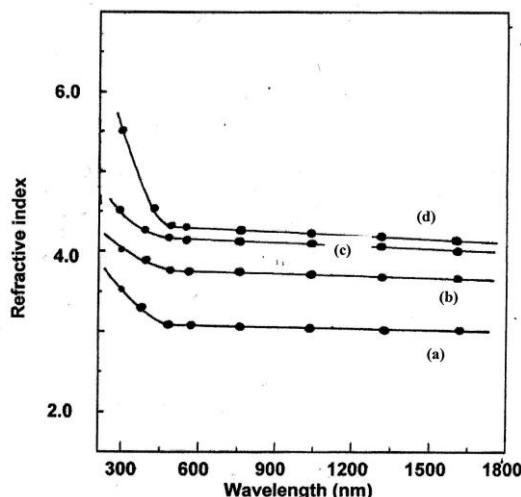


Figure.4 - Variation of refractive index with wavelength of ZnS films deposited at different duty cycles (a) 6% (b) 15% (c) 33% (D) 50%

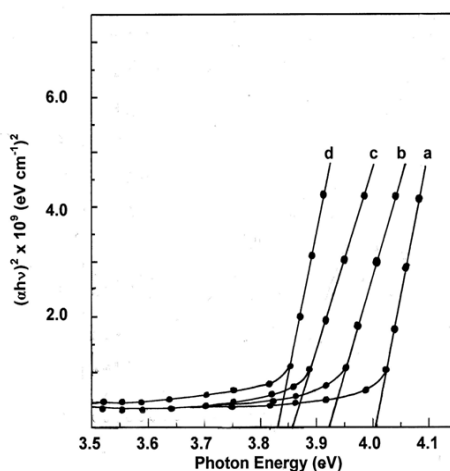


Figure.5 – Tauc’s plot of ZnS films deposited at different duty cycles (a)50 % (b) 33 % (c) 15 % (d) 6 %

In transparent region, the relation between the optical dielectric constant, ϵ_1 , the wavelength, λ , and the refractive index, n , is given by the following equation [20] :

$$\epsilon_1 = n^2 = \epsilon_L - D \lambda^2 \dots\dots\dots(7)$$

where ϵ_1 is the real part of the dielectric constant, ϵ_L is the lattice dielectric constant or (the high-frequency dielectric constant) and D is a constant depending on the ratio of carrier concentration to the effective mass;

$$D = (e^2 N) / (4\pi^2 \epsilon_0 m^* c^2) \dots\dots\dots(8)$$

where ‘e’ is the charge of the electron, N is the free charge carrier concentration, ϵ_0 is the permittivity of free space, m^* is the effective mass of the electron and c is the velocity of light [21] . Fig. 7. shows the relation between n^2 and λ^2 for the ZnS thin films deposited at different duty cycles. It is observed that the dependence $\epsilon_1 (= n^2)$, on λ^2 is linear at longer wavelengths. Extrapolating the linear part of this dependence to zero wavelength gives the value of ϵ_L and from the slope of this linear part, the constant D can be obtained, from which the value (N / m^*) for the thin films can be obtained (Table-3).

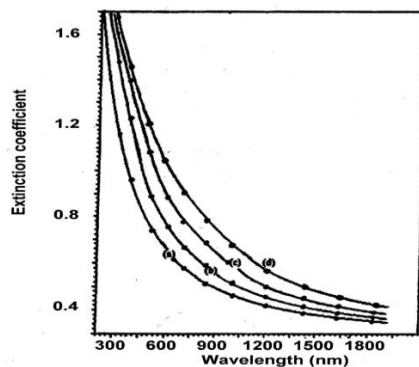


Figure.6 - Variation of extinction co-efficient with wavelength of ZnS films deposited at different duty cycles (a) 6 % (b) 15 % (c) 33 % (d) 50 %

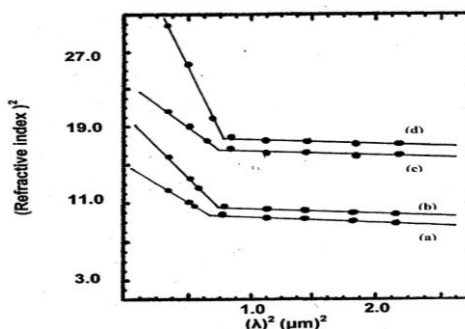


Figure.7 – Variation of (refractive index)² with (wavelength)² of ZnS films deposited at different duty cycles (a) 6 % (b) 15 % (c) 33 % (d) 50 %

According to the single-effective oscillator model proposed by Wemple and DiDomenico [22], the optical data can be described by an excellent approximation using the relation

$$n^2 - 1 = (E_d E_0) / (E_0^2 - E^2) \dots\dots\dots(9)$$

where $E = h\nu$ is the photon energy, n is the refractive index, E_0 is the single-effective oscillator energy and E_d is the dispersion energy which is a measure of the average strength of the interband optical transitions. Plotting $(n^2 - 1)^{-1}$ against E^2 gives the oscillator parameters by fitting a straight line. Figure 8 shows the plot of $(n^2 - 1)^{-1}$ vs E^2 for the films deposited at different duty cycles. The values of E_0 and E_d can then be calculated from the slope $(E_0 E_d)^{-1}$ and the intercept on the vertical axis (E_0/E_d). The values of the static refractive index (n_0) can be calculated by extrapolating the Wemple–DiDomenico dispersion equation (8) to $E \rightarrow 0$. The calculated values of n_0 are 3.0, 3.8, 4.2 and 4.3, for the films deposited at different duty cycle. The calculated values of n_0 , E_0 and E_d are listed in Table 3. In addition, the optical band gap (E_g) determined from the Wemple–DiDomenico dispersion parameter E_0 using the relation $E_g = E_0/2$, are also in good agreement with the band gap values determined from the $(\alpha h\nu)^2$ vs $h\nu$ plot of Fig.5.

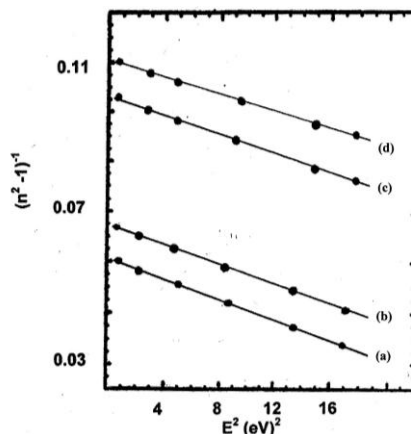


Figure.8 – Variation of $(n^2 - 1)^{-1}$ versus (Photon Energy)² for ZnS films deposited at different duty cycles (a) 50 % (b) 33 % (c) 15 % (d) 6 %

M_{-1} and M_{-3} Moments of the Optical Spectra for the ZnS thin films were obtained from the following relations [23],

$$E_0^2 = M_{-1} / M_{-3} \dots\dots\dots(10)$$

$$E_d^2 = M_{-1}^3 / M_{-3} \dots\dots\dots(11)$$

The single-oscillator parameters E_0 and E_d are related to the imaginary component ϵ_i of the complex dielectric constant. Thus, determining the moments is very important for developing optical applications of the optical material. The obtained values are given in Table 3. The obtained M_{-1} and M_{-3} moments increased with duty cycle.

Table 3The values of single oscillator energy (E_0), dispersion energy (E_d) and optical band gap (E_g) for the ZnS films deposited at different duty cycles

Duty cycle (%)	n_o	E_0 (eV)	E_d (eV)	E_g (eV)	M_{-1}	M_{-3} (eV) ²	$N/m^3 \times 10^{46}$ ($cm^{-3} gm^{-1}$)
6	3.00	7.66	61.28	3.83	8.00	0.14	0.122
15	3.80	7.72	111.50	3.86	14.43	0.24	0.215
33	2.79	7.84	138.29	3.92	17.63	0.29	0.367
50	2.84	8.02	148.28	4.01	18.49	0.30	0.611

IV. Conclusions

In this study, the effect of annealing on the structural, optical, and electrical properties of amorphous ZnS thin films deposited by a chemical bath deposition method has been investigated. X-ray diffraction analysis indicated that as-deposited ZnS films were amorphous, and heat treatments improved slightly the amorphous structure. The Raman spectra of annealed ZnS samples showed first-, second-, and third-order Raman phonons and their compositions. Also, all the films have a direct bandgap, and it decreased from 4.01 to 3.74eV with an increase in annealing temperature. These values are in good agreement with the literature.

References

- [1]. R.Maity and K.K.Chattopadhyay, Synthesis and optical characterization of ZnS and ZnS:Mn nanocrystalline thin films by chemical route, Nanotechnology, 15(7), 2004, 812 - 816.
- [2]. Y.T.Nien, I.G.Chen, C.S.Hwang and S.Y.Chu, Copper concentration dependence of structure, morphology and optical properties of ZnS:Cu,Cl phosphor powder, J.Phys.Chem.Solids, 69 (2-3), 2008, 366- 371
- [3]. T.Nakada, K.Furumi, and A.Kunioka, High efficiency cadmium free CuInGa)Se₂ thin film solar cells with chemically deposited ZnS buffer layers, IEEE Trans.Electron.Devices, 46 (10), 1999, 2093 - 2097
- [4]. A.Fujii, H.Wada, K.I.Shibata, S.Nakayama, M.Hasegawa, In:R.W.Tustison (Ed.), Window and Dome Technologies and Materials VII, SPIE, Bellingham, 2001, p206.
- [5]. F.Göde and C.Gumus, Influences of copper and manganese concentrations on the properties of polycrystalline ZnS:Cu and ZnS:Mn thin films, Optoelectron. Adv. Mat.11 (3), 2009, 429 - 436.
- [6]. A.Klausch, H.Althues, C.Schrage, P.Simon, A.Szatkowski, M. Bredol, D.Adam and S.Kaskel, Preparation of luminescent ZnS:Cu nanoparticles for the functionalization of transoanero acrylate polymers, J.Lumin.130 (4),2010, 692 -697.
- [7]. X.J.Zheng, Y.Q.Chen, T.Zhang, B.Yang, C.B.Jiang, B.Yuan and Z.Zhu, Photoconductive semiconductor switch based on ZnS nanobelt film, Sens. Actuators B147 (2), 2010, 442 - 446.
- [8]. J.Hu, G.Wang, C.Guo, D.Li, L.Zhang and J. Zhao, Au catalyst growth and photoluminescence of zinc blende and wurtzite ZnS nanobelts via chemical vapour deposition, J.Lumin,122-123,2007, 172 - 175.
- [9]. C.Wang, Y.Ao., P.Wang, S. Zhang, J.Qian and J. Hou, A simple method for large scale preparation of ZnS nanoribbon films and its photocatalytic activity for dye degradation, Appl.Surf.Sci, 256 (13), 2010, 4125 - 4128.
- [10]. F.Göde, C.Gumus and M.Zor, Influence of the thickness on physical properties of chemical bath deposited hexagonal ZnS thin films, Optoelectron.Adv.Mater, 9 (7), 2007, 2186 - 2191.
- [11]. K.R.Murali, S.Vasanth and K.Rajamma, Properties of pulse plated ZnS films, Mater.Lett, 62 (12 -13), 2008, 1823 - 1826.
- [12]. M.Ghaemi and L.Binder, Effect of direct and pulse current of Manganese dioxide, J. Power Sources 111 (2), 2002, 248 - 254
- [13]. A.Marlot, P.Kern and L.D. andolt, Pulse plating of Ni-Mo alloys from Ni rich electrolytes, Electrochim. Acta 48 (1),2002, 29 - 36.
- [14]. M.E.Bahrololoom and R.Sani, The influence of pulse plating parameters on the hardness and wear resistance properties of Ni-alumina coatings, Surf.Coat.Tech, 192 (2 -3), 2005, 154 - 163
- [15]. Y.M.Yin, Duplex diffusion layer model with pulse reversal Surf. Coat.Technol., 88 (1 -3),1996,162-164
- [16]. H.McMurdie, M.Morris, E.Evans, B.Paretzkin, W.Wong-Ng and Ettlinger, Standard X-Ray Diffraction Powder Patterns from the JCPDS Research Associateship Hubbard, Powder Diffr. 1 (1), 1986, 64 - 77
- [17]. K.M.Youssef, P.S.Fedkiw and C.C.Koch, Influence of Additives and Pulse Electrodeposition Parameters on Production of Nanocrystalline Zinc from Zinc Chloride Electrolytes, J. Electrochem. Soc. 151 (2), 2004, C103 - C 111
- [18]. H.Karaagac, M. Kaleli and M.Parlak, Characterization of AgGa_{0.5}In_{0.5}Se₂ films deposited by electron beam evaporation, J. Phys. D Appl. Phys. 42 (6), 2009 , 165413.
- [19]. F.Göde, Annealing temperature effect on the structural, optical and electrical properties of ZnS thin films Phys.B, 406 (9), 2012, 1653 - 1659
- [20]. J.M.Gonzalez-Leal, A.Ledesma, A.M.Bernal-Oliva, R.Prieto-Alcon, E.Marquez, J.A.Angel and J.Carabe, Optical properties of thin-film ternary Ge₁₀As₁₅Se₇₅ chalcogenide glasses, Materials Letters, 39 (4), 1999, 232- 239
- [21]. P.O.Edward, Hand Book of Optical Constants of Solids), Academic Press, New York, 1985, p 265.
- [22]. S.H.Wemple and M. DiDomenico, Behaviour of the electronic dielectric constant in covalent and ionic materials, Phys. Rev. B3 (4), 1971, 1338 - 1350
- [23]. M.S.Kim., K.G.Yim, J.Son and J.Y.Leem, Effects of Al Concentration on Structural and Optical Properties of Al-doped ZnO, Thin Films, Bull.Kor.Chem Soc 33 (4), 2012, 1235 - 1241.